Resolving Mechanisms of Competitive Fertilization Success in Drosophila melanogaster

Mollie K. Manier, *et al.*

Science **328**, 354 (2010);
DOI: 10.1126/science.1187096

30. D. Bachtrog, *Curr. Opin. Genet. Dev.* **16**, 578 (2006).

31. We thank D. Kirk for DNA from *Volvox* mapping populations. We thank V. Lundblad and S. Merchant for advice on the manuscript. This work was supported by the Coypu Foundation and from grants NIH R01 GM078376 to J.G.U.; NIH F32 GM086037 to B.O.; Japan Society for the Promotion of Science grant S05750/L06701 to P.F.; Grant-in-Aid for Scientific Research (20247032) from the Ministry of Education, Culture, Sports, Science and Technology, Japan to H.N.; NIH grant T32-HG002536 to S.D.; and DE-FC02-02ER63421 and AFOSR to M.P. DOE-JGI provided sequencing and analyses for algal mating loci under the Community Sequencing Program (776835) supported by the Office of Science of DOE under contract DE-AC02-05CH11231. Sequencing of the *V. carteri* genome was performed under the auspices of DOE's Office of Science, Biological and Environmental Research Program and by the University of California, Lawrence Berkeley National Laboratory under contract DE-AC02-05CH11231, Lawrence Livermore National Laboratory under contract DE-AC52-07NA27344, and Los Alamos National Laboratory under contract DE-AC02-06NA25396. Sequences generated in this study have been deposited in GenBank under accession numbers GU814014, GU814015, GU784915, GU784916, and GU735444-GU735478. Materials used in this study will be made available upon request with the completion of a Materials Transfer Agreement from Salk Institute.

Supporting Online Material

www.sciencemag.org/cgi/content/full/328/5976/351/DC1
Materials and Methods
SOM Text
Figs. S1 to S17
Tables S1 to S15
References

22 December 2009; accepted 12 March 2010
10.1126/science.1186222

Resolving Mechanisms of Competitive Fertilization Success in *Drosophila melanogaster*

Mollie K. Manier, John M. Belote, Kirstin S. Berben, David Novikov, Will T. Stuart, Scott Pitnick*

Our understanding of postcopulatory sexual selection has been constrained by an inability to discriminate competing sperm of different males, coupled with challenges of directly observing live sperm inside the female reproductive tract. Real-time and spatiotemporal analyses of sperm movement, storage, and use within female *Drosophila melanogaster* inseminated by two transgenic males with, respectively, green and red sperm heads allowed us to unambiguously discriminate among hypothesized mechanisms underlying sperm precedence, including physical displacement and incapacitation of "resident" sperm by second males, female ejection of sperm, and biased use of competing sperm for fertilization. We find that competitive male fertilization success derives from a multivariate process involving ejaculate-female and ejaculate-ejaculate interactions, as well as complex sperm behavior in vivo.

Remating with different males by females generates sexual conflict over paternity (*1*) and sets the stage for postcopulatory sexual selection (*2*–*4*), which can drive diversification of both male and female biochemistry, physiology, morphology, and behavior (*4*, *5*). Most investigations of postcopulatory sexual selection have focused on the pattern of sperm precedence, such as the proportion of progeny sired by the second of two males subsequent to female remating (P_2). However, without knowledge of underlying mechanisms, these patterns reveal little about the intensity of selection or sex-specific adaptation (*4*–*6*). Consequently, even with *Drosophila melanogaster*, there is contention over the mechanisms giving rise to the roughly 80% last-male sperm precedence observed (*7*–*12*). Our understanding of these and other phenomena has been constrained by the technical challenge of directly observing sperm dynamics within the female reproductive tract and our limited ability to discriminate between sperm of different males (*7*, *13*, *14*).

We have overcome these challenges by transforming *D. melanogaster* to express a protamine labeled with green fluorescent protein (GFP) or red fluorescent protein (RFP) in sperm heads, which can be easily observed and unambiguously differentiated within the female reproductive tract (figs. S1 and S2 and movies S1 to S3). These lines enable direct visualization of sperm competition in vivo, in real time, and over extensive periods of time, allowing us to discriminate among alternative hypothesized mechanisms of sperm precedence. Multiple indices of male fitness relevant to sperm and/or ejaculate function were assayed, with transgenic males compared with each other and with a wild-type LH_m strain (into which the GFP and RFP constructs were backcrossed for six generations). Although some significant differences were found, with transformed lines performing less well, equivalent to, or better than the wild type in different fitness assays, all three strains fell within the typical range of values reported in the literature for all assays (figs. S3 to S7), which suggested there was no dysfunction of transformant sperm. Moreover, results of the sperm precedence experiments reported below are unbiased, because GFP and RFP males (i) were competed using a reciprocal mating order design and (ii) did not differ in female remating interval, P_1, or P_2 in those experiments (*15*).

We quantified (i) spatiotemporal patterns of sperm storage and use by the female after remating, (ii) the extent and timing of sperm ejection by females, and (iii) the influence of remating on resident sperm motility. Unless otherwise specified, in all experiments, 3-day-old, virgin LH_m females were randomly assigned to all treatment groups, initially mated to a GFP or an RFP male, and, beginning 3 days later (the typical remating latency for *D. melanogaster*), provided a daily, 6-hour opportunity to remate to a male of the alternative genotype (reciprocal male mating order balanced). All copulations were observed, and copulation durations recorded (*15*).

Department of Biology, Syracuse University, Syracuse, NY 13244–1270, USA.

*To whom correspondence should be addressed. E-mail: sspitnic@syr.edu

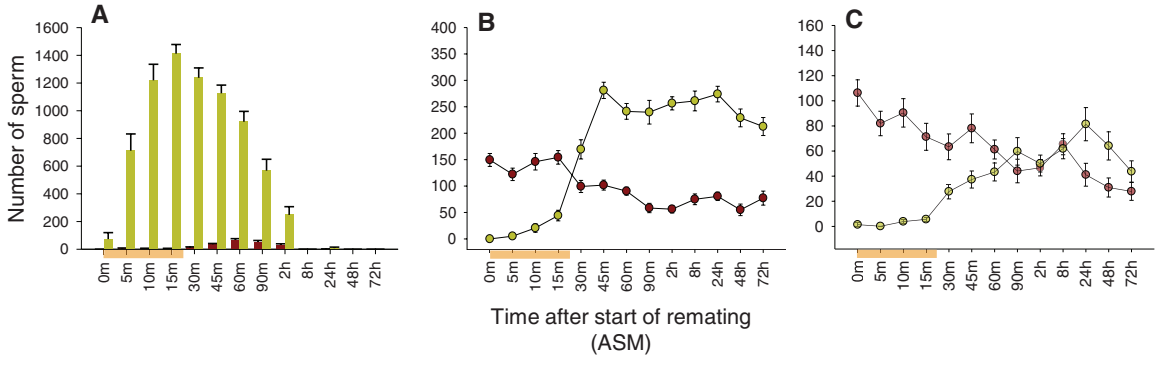

Fig. 1. Numbers of first-male (red) and second-male (yellow) sperm in the (**A**) bursa, (**B**) seminal receptacle, and (**C**) spermathecae for 13 time points ASM, averaged over two experimental replicates and both reciprocal mating orders. Error bars represent SEM.

To quantify temporal dynamics of sperm fate, females in two experimental replicates were flash-frozen at randomly assigned times after the start of the second mating (ASM): 0 min (immediately after second male mounting), 5 min, 10 min, 15 min, 30 min, 45 min, 60 min, 2 hours, 8 hours, and 24 hours, with three additional time points in the second replicate: 90 min, 48 hours, and 72 hours. For the last three time treatments of the second replicate (24 hours, 48 hours, 72 hours), all progeny were reared, and the proportion sired by the second male (P_2) was determined by assaying all sons for green or red sperm. Frozen females were dissected, and red and green sperm were counted in the bursa (the site of insemination), paired spermathecae (including spermathecal ducts), and the seminal receptacle (SR), distinguishing between the proximal and distal halves. For illustrative purposes, results from both replicates and male mating orders are combined in Fig. 1 [individual replicates and male mating orders shown in figs. S8 to S10; see (*15*) for tests of differences], with sample sizes per time treatment ranging from 30 to 50 females (total $N = 543$) (table S1).

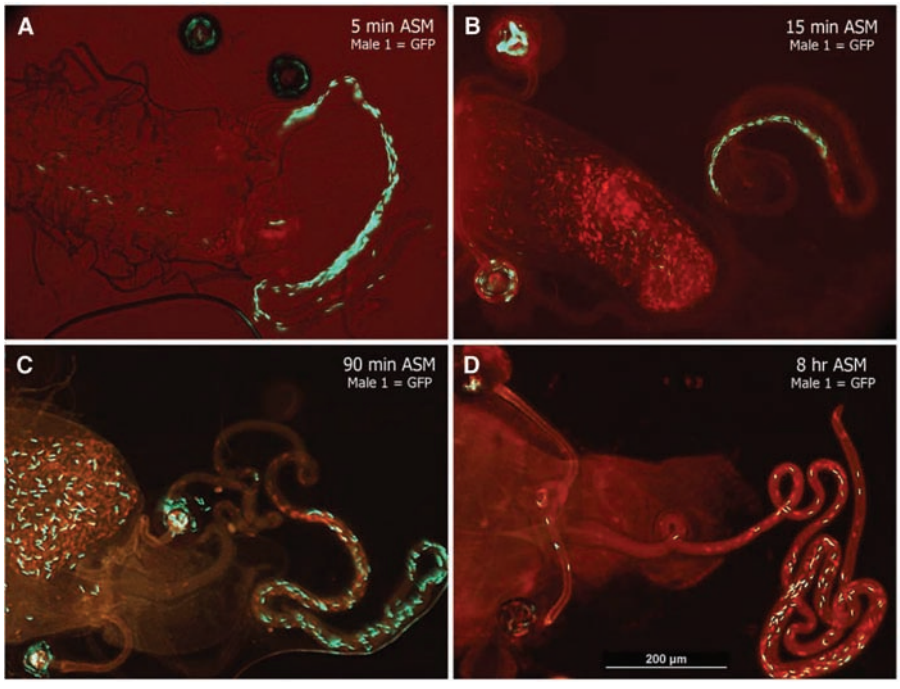

Fig. 2. Representative female reproductive tracts at (**A**) 5 min, (**B**) 15 min, (**C**) 90 min, and (**D**) 8 hours ASM, showing relative abundances and locations of first-male (GFP) and second-male (RFP) sperm.

Fig. 3. Ejected sperm mass containing both first-male (GFP) and second-male (RFP) sperm under (**A**) differential interference contrast and (**B**) fluorescence.

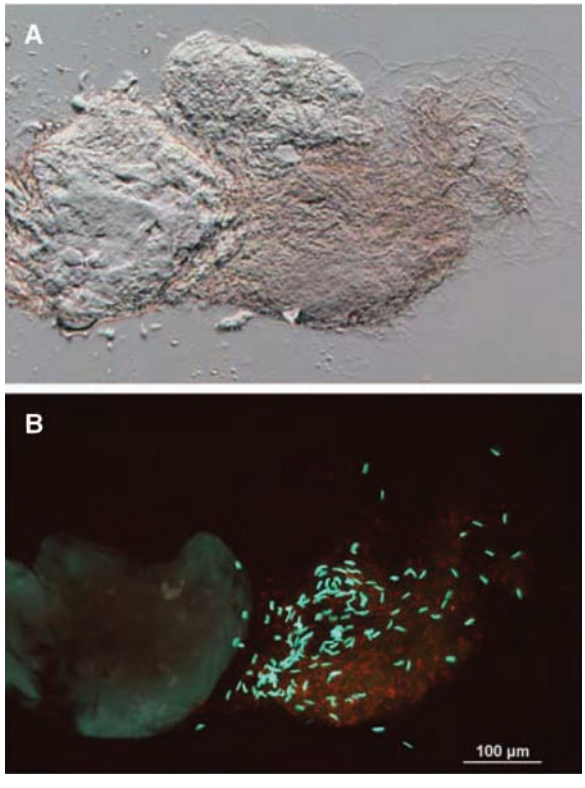

We revealed two different mechanisms by which resident sperm are displaced from the sperm-storage organs after remating and which contribute to last-male sperm precedence. First, there was an early release of some resident sperm from storage into the bursa, a process that does not involve second-male sperm. Second, resident sperm appear to have been physically displaced over time from both the SR and the spermathecae by incoming second-male sperm. Wild-type females store ~400 sperm at maximum in their SR and 130 sperm in the paired spermathecae (Fig. 1). Upon remating (i.e., time 0 ASM), resident sperm were depleted from this maximum capacity, because sperm were used for fertilization over the preceding days to 149 (± 12) sperm in the SR and 108 (± 11) sperm in the spermathecae. Resident sperm were rarely observed in the bursa (Fig. 1) or in the spermathecal ducts at time 0. Insemination of second-male sperm began as early as 5 min ASM (25 out of 46 cases or 54% of the time), and in 19% of cases where second-male sperm had not yet been transferred (5 out of 26), some resident sperm (17 ± 5) were observed in the bursa 5 to 10 min ASM (Figs. 1 and 2). We also saw first-male sperm in the bursa in 14% of observations where second-male sperm had been transferred but had not yet entered storage (5 out of 37). This release of resident sperm was presumptively female mediated and triggered by male accessory gland proteins (Acps) and/or mechanical stimulation of copulation.

First-male sperm continued to be displaced as second-male sperm entered storage, soon after insemination (the SR earlier than the spermathecae) (Fig. 1) (*16*). Sperm transfer peaked at 15 min ASM (1412 ± 66 sperm, or ~2.7 times the female's storage capacity), after which second-male sperm steeply declined in the bursa, while resident sperm steadily increased. Although sperm storage leveled off around 45 min ASM, the first- and second-male sperm proportions continued to change, with displacement peaking 60 to 90 min ASM (Fig. 1), when 26% of resident stored sperm had been relocated into the bursa. Although this process is likely to displace some of the second male's own sperm (*17*), it will also increase the proportion of second-male sperm in storage (as observed) because of their overrepresentation in the bursa. This outcome also depends on active motility within the storage organs (movies S1 to S3) and adequate mixing of first- and second-male sperm, consistent with our observations (fig. S11 and movies S4 and S5). Competing sperm were highly stratified during and immediately after

copulation, with resident sperm concentrated in the distal half of the SR (Fig. 2, B and C), but dynamic mobility of sperm in storage increased mixing over time (Fig. 2D and fig. S11).

The question of why males ejaculate many more sperm than can be stored has long puzzled researchers, given that the (1.8 mm) sperm of *D. melanogaster* are many times longer than any distance they travel within the female and that storage appears to be a rapid and efficient process (*18*). We postulate that excess sperm and, perhaps, their mobility (movie S6) are adaptations to sperm competition in this species, specifically to physical displacement of resident sperm. Indeed, the size of the second male's ejaculate was significantly correlated with the amount of resident sperm displaced from storage, and the strength of this relation increased substantially between 45 and 60 min ASM (fig. S12) [45 min ASM: $n = 45$, $F_{1, 43} = 6.85$, coefficient of determination (R^2) = 0.137, $P = 0.012$; 60 min ASM: $n = 34$, $F_{1, 32} = 30.95$, $R^2 = 0.49$, $P < 0.0001$]. These results also suggest that ejaculate size is evolving via sexual selection mediated by sperm competition.

Sperm storage and displacement dynamics cease when the female ejects excess second-male and displaced first-male sperm from her reproductive tract. To establish that females are ejecting sperm, as previously inferred (*13*), we doubly mated wild-type females to GFP and RFP males and, within 30 min after copulation, transferred females in groups of up to five (mean = 4.7) into 20 cubes constructed of glass coverslips. Cubes were deconstructed 3 hours later, and the coverslips were examined under fluorescence. We found several ejected sperm masses per cube, highly stereotypical in form (Fig. 3), consisting of mixed (but predominantly second-male) sperm in association with the gelatinous mating plug. To better quantify ejection, wild-type females were isolated in glass three-well spot plates beneath coverslips immediately after mating to GFP males, and we checked for ejection every 10 min for up to 5 hours using a stereomicroscope. Ejected masses were immediately transferred to saline on slides and examined under epifluorescence to confirm the presence of GFP sperm, and females were dissected to examine the bursa for sperm. We found that 84% of females ($n = 61$) ejected sperm within five hours of mating (181 ± 11 min, mean ± SEM), and none of these females had any sperm in their bursa, nor had they laid any eggs. Additionally, on examination, first eggs laid in media vials in the time-series experiment (above) were never associated with large amounts of sperm, which suggests that active sperm ejection by females is typical, if not universal.

After ejection, remaining stored sperm make up the "fertilization set" (*19*) or the population of sperm directly engaging in sperm-sperm competition. To delineate which storage organs house the fertilization set, we compared simple linear regressions of P_2 on the proportion of second-male sperm in storage (S_2) (Fig. 4) (*15*). S_2 was found to be a highly significant predictor of P_2 for the SR ($F_{1, 73} = 25.55$, $P < 0.0001$, $R^2 = 0.259$) but not the spermathecae ($F_{1, 70} = 0.26$, $P = 0.614$, $R^2 = 0.004$), reinforcing previous indirect evidence (*20*) that sperm in the SR constitutes the more immediate fertilization set. Proportional representation in the proximal versus distal regions of the SR may further contribute to differential fertilization success and has been shown to be influenced by sperm length (*21*, *22*). However, sperm length here did not systematically vary between first and second males, and sperm proportions did not differ regionally in the SR in the hours immediately after mating (fig. S11).

We finally tested if each male's sperm in the SR post ejection was equally competitive, akin to a "fair raffle" (*19*), with sperm used for fertilization in direct proportion to their prevalence. Two results suggest that they were: (i) in vivo sperm motility did not change upon remating and (ii) sperm were used in direct proportion to their abundance. First, we examined if female remating induces a change in motility of GFP resident sperm in the SR, by quantifying their velocity and percent motility (i) 5 min ASM to an RFP male, (ii) 60 min ASM to an RFP male, (iii) 60 min after the first mating, and (iv) 3 days after the first mating (*15*). Percent motility and sperm velocity showed no significant changes, which suggested that in the SR, neither several days of storage nor female remating had any detrimental effect on sperm survival or motility (fig. S13 and movies S5 and S6). Second, if sperm competition was disproportionately and systematically biased toward one male over another ("loaded raffle"), the slope of the regression of P_2 on S_2 would be either significantly less than 1 (favoring the first male) or greater than 1 (favoring the second male). However, the slope of the reduced major axis regression was not significantly different from 1 [slope = 1.203, $t(68) = 0.81$, $P = 0.422$] (Fig. 4A), which supported the fair-raffle hypothesis.

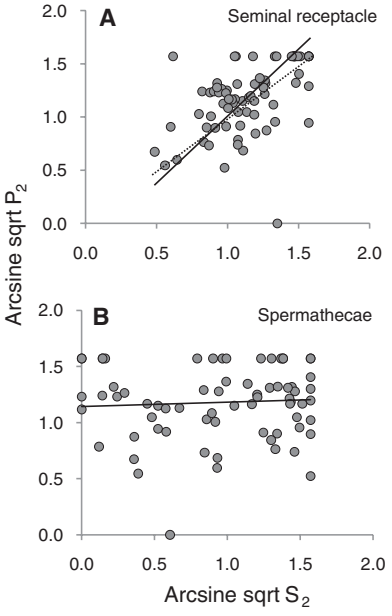

Fig. 4. Relation between P_2 and S_2 (both variables arcsine square root transformed) in the (**A**) seminal receptacle and (**B**) spermathecae. Seminal receptacle: $y = 1.203x - 0.191$ (reduced major axis regression); spermathecae: $y = 0.0383x + 1.144$ (simple linear regression).

Our observations of in vivo motility and fine-scale spatiotemporal patterns of sperm fate corroborate some previously conjectured mechanisms underlying competitive fertilization success, including sperm displacement (*10*, *12*, *23*) and sperm ejection by females (*13*), but fail to support other proposed mechanisms, such as sperm incapacitation (*9*–*11*). We cannot exclude the possibility that Acp-mediated incapacitation contributes to the early release of some resident sperm from storage. However, we would then expect to see dead or dying sperm in storage and in the bursa, yet neither sperm velocity nor sperm motility in storage changed upon remating. Our results complement other investigations of sperm mortality of competing ejaculates in vivo (*13*) and in vitro (*24*), which suggested that incapacitation makes little to no contribution to sperm precedence in *D. melanogaster*. The present investigation reveals that postcopulatory sexual selection in *D. melanogaster* includes the early release of resident sperm from storage, the heterogeneous distribution of competing sperm proportions in different storage organs, fair-raffle sperm use in the SR, and the surprising level of sperm mobility within female sperm-storage organs (movies S1 to S5). Most important, a complex and dynamic array of processes underlying patterns of sperm precedence (e.g., P_2) can now be dissected in targeted, detailed genetic analyses to reveal specific behavioral, physiological, and biochemical mechanisms relevant to postcopulatory sexual selection.

References and Notes

1. G. A. Parker, in *Sexual Selection and Reproductive Competition in Insects*, M. S. Blum, N. A. Blum, Eds. (Academic Press, New York, 1979), pp. 123–166.
2. G. A. Parker, *Biol. Rev. Camb. Philos. Soc.* **45**, 525 (1970).
3. W. G. Eberhard, *Female Control: Sexual Selection by Cryptic Female Choice* (Princeton Univ. Press, Princeton, NJ, 1996).
4. T. R. Birkhead, A. P. Møller, *Sperm Competition and Sexual Selection* (Academic Press, London, 1998).
5. T. R. Birkhead, D. J. Hosken, S. Pitnick, *Sperm Biology: An Evolutionary Perspective* (Academic Press, London, 2009).
6. A. Bjork, S. Pitnick, *Nature* **441**, 742 (2006).
7. A. Bjork, W. T. Starmer, D. M. Higginson, C. J. Rhodes, S. Pitnick, *Proc. Biol. Sci.* **274**, 1779 (2007).
8. T. Pizzari, G. A. Parker, in *Sperm Biology: An Evolutionary Perspective*, T. R. Birkhead, D. J. Hosken, S. Pitnick, Eds. (Academic Press, London, 2009), pp. 207–245.
9. A. Civetta, *Curr. Biol.* **9**, 841 (1999).
10. C. S. C. Price, K. A. Dyer, J. A. Coyne, *Nature* **400**, 449 (1999).
11. L. G. Harshman, T. Prout, *Evolution* **48**, 758 (1994).
12. A. S. Gilchrist, L. Partridge, *J. Insect Physiol.* **41**, 1087 (1995).
13. R. R. Snook, D. J. Hosken, *Nature* **428**, 939 (2004).

14. A. D. Stewart, A. M. Hannes, W. R. Rice, *Evolution* **61**, 636 (2007).
15. Materials, methods, supplementary analyses, and discussion are available as supporting material on *Science* Online.
16. E. M. Adams, M. F. Wolfner, *J. Insect Physiol.* **53**, 319 (2007).
17. G. A. Parker, L. W. Simmons, *Proc. Biol. Sci.* **246**, 107 (1991).
18. K. Ravi Ram, M. F. Wolfner, *Integr. Comp. Biol.* **47**, 427 (2007).
19. G. A. Parker, in *Sperm Competition and the Evolution of Animal Mating Systems*, R. L. Smith, Ed. (Academic Press, Orlando, FL, 1984), pp. 1–60.
20. S. Pitnick, T. A. Markow, G. S. Spicer, *Evolution* **53**, 1804 (1999).
21. J. M. Pattarini, W. T. Starmer, A. Bjork, S. Pitnick, *Evolution* **60**, 2064 (2006).
22. G. T. Miller, S. Pitnick, *Science* **298**, 1230 (2002).
23. G. Lefevre Jr., U. B. Jonsson, *Genetics* **47**, 1719 (1962).
24. L. Holman, *Funct. Ecol.* **23**, 180 (2009).
25. Supported by the NSF (grants DEB-9806649 and DEB-0814732). We thank S. McClear for assistance with the protamine constructs and M. Wong for technical assistance.

Supporting Online Material
www.sciencemag.org/cgi/content/full/science.1187096/DC1
Materials and Methods
SOM Text
Figs. S1 to S13
Table S1
References
Movies S1 to S6

14 January 2010; accepted 3 March 2010
Published online 18 March 2010;
10.1126/science.1187096
Include this information when citing this paper.

Structural Basis of Preexisting Immunity to the 2009 H1N1 Pandemic Influenza Virus

Rui Xu,[1]* Damian C. Ekiert,[1]* Jens C. Krause,[2] Rong Hai,[3] James E. Crowe Jr.,[2] Ian A. Wilson[1,4]†

The 2009 H1N1 swine flu is the first influenza pandemic in decades. The crystal structure of the hemagglutinin from the A/California/04/2009 H1N1 virus shows that its antigenic structure, particularly within the Sa antigenic site, is extremely similar to those of human H1N1 viruses circulating early in the 20th century. The cocrystal structure of the 1918 hemagglutinin with 2D1, an antibody from a survivor of the 1918 Spanish flu that neutralizes both 1918 and 2009 H1N1 viruses, reveals an epitope that is conserved in both pandemic viruses. Thus, antigenic similarity between the 2009 and 1918-like viruses provides an explanation for the age-related immunity to the current influenza pandemic.

Influenza pandemics in humans tend to occur decades apart and infect a large percentage of the human population with substantial mortality. In the 20th century, three pandemics were caused by the emergence of different influenza A subtypes that were antigenically divergent from human viruses circulating at the time: 1918 H1N1 ("Spanish flu"), 1957 H2N2 ("Asian flu"), and 1968 H3N2 ("Hong Kong flu") (*1*). Since April 2009, the outbreak of a novel influenza A H1N1 virus (2009 H1N1) in Mexico has spread globally and developed into the first human influenza pandemic in 40 years. The 2009 H1N1 virus has now infected the human population worldwide and contributed to at least 16,000 deaths as of 26 February 2010 (*2*).

The influenza virus envelope protein, hemagglutinin (HA), is the principal surface antigen (*3*) and the most critical component of flu vaccines (*4*). At the beginning of a flu pandemic, preexisting immunity to the HA of the newly emerging virus is generally low, guaranteeing a large pool of susceptible hosts for rapid spread and infection of 10 to 40% of the population worldwide. After a new HA becomes fixed in circulating human viruses, it undergoes gradual changes in its antigenic structure in a process called antigenic drift, so as to escape recognition by the human immune system. Such drift leads to loss of immunity and is associated with the frequent flu epidemics that occur during interpandemic periods.

The 2009 pandemic virus HA originated from the swine lineage of H1 HAs and closely resembles that of current circulating H1 viruses in swine (Fig. 1A) (*5*–*7*), whereas seasonal human H1 HAs diverged from the swine lineage early in the 20th century (*8*). Descendants of the human 1918 H1N1 virus continued to circulate

[1]Department of Molecular Biology, Scripps Research Institute, 10550 North Torrey Pines Road, La Jolla, CA 92037, USA. [2]Departments of Pediatrics and Microbiology and Immunology, Vanderbilt University Medical Center, Nashville, TN 37232, USA. [3]Department of Microbiology, Mount Sinai School of Medicine, New York, NY 10029, USA. [4]Skaggs Institute for Chemical Biology, Scripps Research Institute, 10550 North Torrey Pines Road, La Jolla, CA 92037, USA.

*These authors contributed equally to this work.
†To whom correspondence should be addressed. E-mail: wilson@scripps.edu

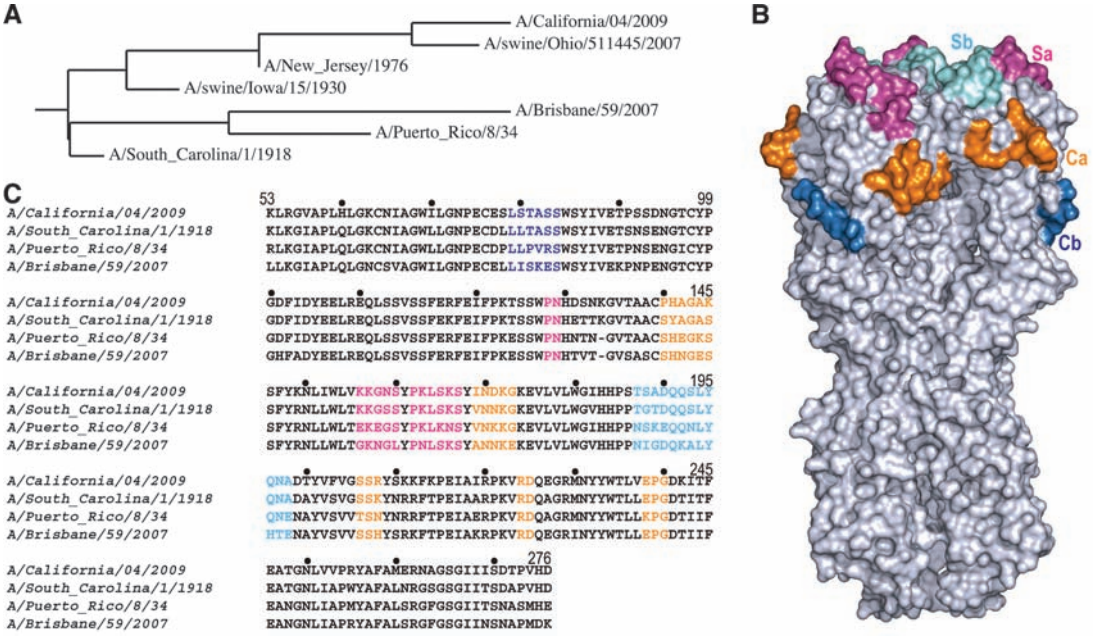

Fig. 1. Crystal structure, phylogeny, and antigenic variation in influenza A 2009 H1N1 HA. (**A**) Phylogenetic tree of selected H1 HAs in swine and human. (**B**) Antigenic structure of CA04 HA from the 2009 H1N1 pandemic virus. A trimer complex is shown in surface representation with the antigenic sites highlighted: Sa site in magenta, Sb site, cyan; Ca site, orange; and Cb site, blue. Sa and Sb sites are located near the receptor-binding site. The Ca site straddles the subunit interface in the trimer. (**C**) Sequence alignment of membrane-distal domains from representative H1 HAs (*38*). Antigenic epitopes are color-coded as in (B).